point. This point represents the maximum possible degree of metastable superheating on a given isotherm, and at $P = 0$ it is about 0.9 T_c. The equilibrium isotherms are horizontal lines in the mixed phase, whose position is determined by equality of the Gibbs potential in the liquid and vapor phases.

For illustration, assume that the material is superheated to the metastable state indicated by the circle in Fig. 1; that is, $P = 1$ bar, $T = 170$ K, and $v = 4.0$ cm^3/g. At this point the internal energy is 320 J/g larger than that at the boiling point, 120 K. The Rankine-Hugoniot curve centered here is labeled *R-H*. Points to the right of the initial volume, $v = 4.0$, are meaningless and are shown as an aid in locating the curve. A shock centered on the assumed initial state whose end state lies on the equilibrium surface in the mixed phase is seen to be restricted to a narrow pressure range at about 28 bars. Moreover, it represents an eigenvalue, or weak, detonation since the shock is supersonic with respect to the material behind; the isentrope through the final shocked state is shown as the curve labeled *S* and clearly has a smaller negative slope than the Rayleigh line, labeled *R* (*6*).

The detonation velocity cannot be evaluated because it is determined by a saddle-point singularity of the differential equation expressing the relation between the specific volume and the reaction rate in the shock transition (*6*). It therefore depends on the values of the reaction rate and viscosity coefficients in the final shocked state, and these are not known. The velocity can be bounded below, however, at about 0.5 mm/μsec.

The pressure decays in the rarefaction wave following the shock along curve *S* until the initial pressure is reached. The temperature at that point is 120 K, the specific volume is 178 cm^3/g, and the internal energy is 225 J/g. The degree of reaction is 0.45. The difference in internal energy between the initial state for the shock and the final state behind the entire wave is therefore (320 − 225) J/g, or 95 J/g. This energy is extracted as mechanical work and is the effective energy of explosion. It is small, as is the detonation pressure, compared to chemical high explosives, for which the energy is typically 4000 J/g. However, it is sufficient to be very hazardous in large quantities, and seems to be compatible with the magnitude of energy release inferred from observed vapor explosions.

Whether detonations are the mechanism for vapor explosions depends not only on the thermodynamic requirements, which are seen to be satisifed, but also on the ability of the shock to be self-sustaining. That is, initiation of the reaction must occur in the shock transition layer. On the basis of equilibrium thermodynamics alone it appears difficult to argue that the shock should be self-sustaining. Thus, the effect of the shock pressure is to carry material closer to the equilibrium surface and farther from the spinodal curve.

It may be possible, however, that nonuniform heating in the shock front causes local high temperatures that initiate the reaction, analogous to the situation in liquid chemical explosives. Small bubbles may nucleate in the metastable liquid and have insufficient time to grow before the shock starts. Shock compression of these bubbles can then cause local high temperatures. It may even be unnecessary for bubbles to have formed. Density fluctuations are large in the vicinity of the spinodal point and corresponding temperature fluctuations of the shocked material may be large.

In any case, definitive experiments are required to establish whether the detonation mechanism obtains, as well as to measure pertinent parameters.

G. R. FOWLES
Physics Department, Washington State University, Pullman 99164

References and Notes

1. L. C. White, J. E. Cox, J. E. Bouvier, *J. Met.* **22**, 39 (1970).
2. E. Nakanishi and R. C. Reid, *Chem. Eng. Prog.* **67**, 36 (1971).
3. W. M. Porteous and R. C. Reid, *ibid.* **72**, 83 (1976).
4. S. A. Colgate and T. Sigureirsson, *Nature (London)* **244**, 552 (1973).
5. M. M. Martynyuk, *Fiz. Goreniya Vzryva* **13**, 213 (1977).
6. R. Rabie, G. R. Fowles, W. Fickett, *Phys. Fluids*, in press.
7. C. Tsonopoulos and J. M. Prausnitz, *Cryogenics* **9**, 315 (1969).
8. *Matheson Gas Data Book* (Matheson Co., East Rutherford, N.J., ed. 4, 1966), p. 315.
9. Supported by the Department of Energy.

14 December 1978

Head-to-Head Linked Isoprenoid Hydrocarbons in Petroleum

Abstract. *A series of petroleum isoprenoid hydrocarbons possessing an unusual head-to-head linkage is present as an important component in petroleum. The entire series appears to be produced by diagenesis or catagenesis from precursors containing 40 carbon atoms. A suitable precursor compound has been reported in one type of living organism, thermoacidophile bacteria.*

While high-molecular-weight hydrocarbons possessing a single tail-to-tail linkage, such as squalane (*1*), perhydro-β-carotene (*2*), and lycopene (*3*) have been reported, all other high-molecular-weight isoprenoids found to date in fossil-fuel samples possess only head-to-tail linkages (*4*). We now report the discovery of head-to-head linked isoprenoid hydrocarbons of high molecular weight in crude oils. This type of linkage was only recently discovered in living organisms (*5*).

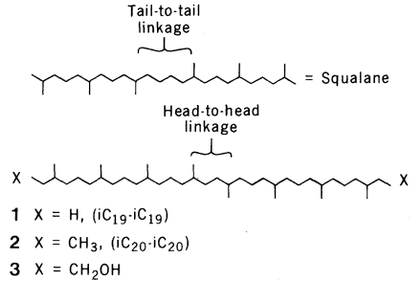

The solid peaks in Fig. 1 depict the head-to-head linked isoprenoids in considerable concentration (0.1 percent of crude) relative to their head-to-tail linked counterparts (shaded peaks).

The head-to-head linkage was discovered by interpretation of capillary gas chromatography–mass spectrometry (GC-MS) (Fig. 2B) of the branched acyclic saturated fraction produced by alumina-silica chromatography (*6*), with subsequent thiourea adduction (*2*) from a California Miocene crude. The diagnostic series of ion doublets (*7*) observed at *m/e* 112–113, 182–183, 252–253, 308–309, 378–379, and 448–449 (Fig. 2B) is indicative of head-to-head linkage, and confirmation was obtained by comparison with authentic head-to-head iC_{19}-iC_{19} (*i*, isoprenoid) (Fig. 2A).

Authentic 2,6,10,14,17,21,25,29-octamethyltriacontane (**1**, iC_{19}-iC_{19}) was synthesized in three steps starting from methylpristanate (Analabs). Lithium

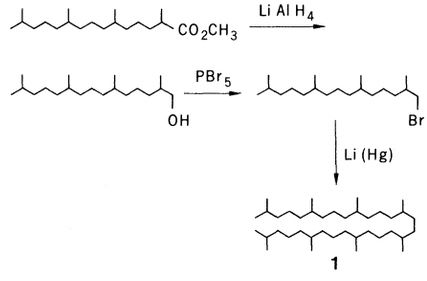

aluminum hydride reduction of the ester to pristanol was followed by conversion to 1-bromopristane by means of phos-

0036-8075/79/0413-0169$00.50/0

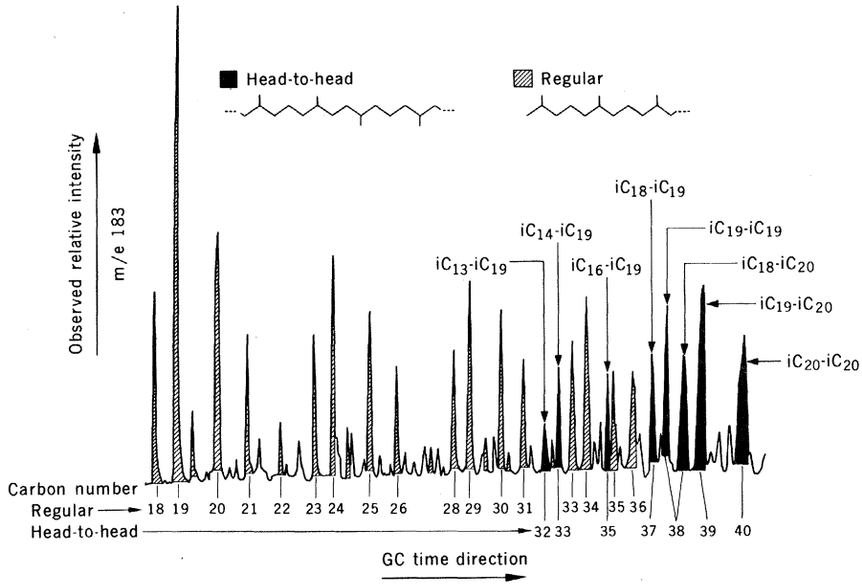

Fig. 1. Mass fragmentogram of isoprenoids of a California Miocene crude, 1535 m in depth. Capillary GC-MS with a 60-m, 0.05-cm (inside diameter) nickel wall-coated Dexsil 400 column (Hewlett-Packard 7620A GC; Nuclide 12-90G MS) at 70 eV.

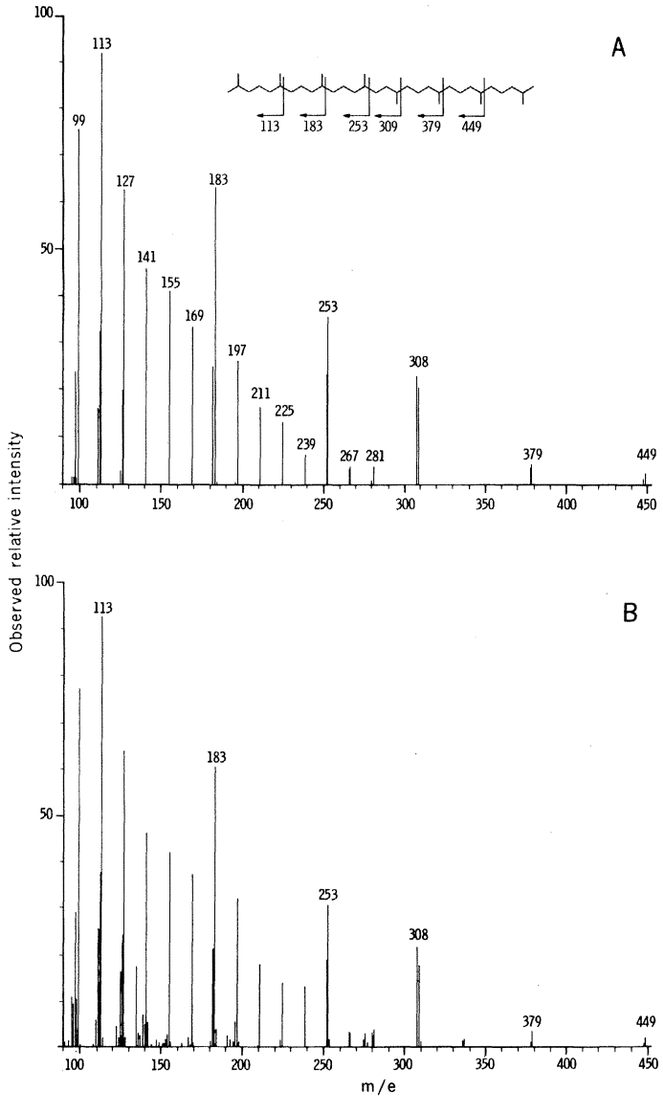

Fig. 2. Proof of structure of an irregular head-to-head isoprenoid in petroleum comparison of mass spectra. (A) Authentic head-to-head iC_{19}-iC_{19}, 1. (B) Head-to-head $iC_{19}iC_{19}$ in a California Miocene crude. Mass spectral conditions are the same as in Fig. 1.

phorus pentabromide in chloroform over sodium carbonate. The 1-bromopristane was coupled in a Wurtz-type reaction by means of lithium amalgam in refluxing dioxane (*8*) to give a 1 percent yield (by GC) of **1** in solution with unreacted bromide. The synthetic iC_{19}-iC_{19} (**1**) coeluted with the natural iC_{19}-iC_{19} peak from petroleum on capillary GC on two different nickel columns, namely, 60-m Dexsil 400 or OV-101 wall-coated, 0.05 cm in inside diameter.

The components detected in petroleum include various combinations of regular iC_{13} through iC_{20} isoprenoids linked head to head with regular iC_{19} or iC_{20} isoprenoids (Fig. 1), the largest homolog being iC_{20}-iC_{20} (**2**). A head-to-head homolog containing a regular iC_{17} isoprenoid portion is conspicuously absent, as is often the case with the regular iC_{17} isoprenoid. These phenomena are reminiscent of the normal diagenesis pattern of phytane (and its precursors) found in crude oil (*3*); that is, all of the lower head-to-head homologs can be considered as diagenetic debris from one or more precursors which contain the iC_{20}-iC_{20} arrangement of carbon atoms.

This same series of head-to-head linked isoprenoids was detected in crude oils and source rock extracts from diverse locations in Canada, Venezuela, the United States, and the U.S.S.R.

The head-to-head structural feature has only one known biological natural product analog, $\omega\omega'$-biphytanediol (**3**), found in cell-wall membranes of thermoacidophile bacteria of the Calderiella series (*5*). Thus, it seems likely that microbial species present during the early stages of catagenesis would contain similar suitable head-to-head linked isoprenoid precursors. Further support for a genetic connection comes from Albrecht (*9*), who has identified several C_{40} head-to-head linked isoprenoids, including **2**, by chemical degradation of kerogen. Previously, bacteriohopane tetrol (C_{35}), which has been found in *Acetobacter xylinum* (*10*), has been linked to C_{31} to C_{35} petroleum hopanes having extended side chains (*11*), another possible genetic relation between microorganisms and petroleum. The discovery of head-to-head linked isoprenoids in petroleum provides compelling evidence for a ubiquitous and substantial contribution of bacterial cell-wall lipids to crude oils.

J. MICHAEL MOLDOWAN
WOLFGANG K. SEIFERT
Chevron Oil Field Research Company,
Post Office Box 1627,
Richmond, California 94802

References and Notes

1. P. M. Gardner and E. V. Whitehead, *Geochim. Cosmochim. Acta* **36**, 259 (1972).
2. M. T. J. Murphy, A. McCormick, G. Eglinton, *Science* **157**, 1040 (1967).
3. B. J. Kimble, J. R. Maxwell, R. P. Philp, G. Eglinton, P. Albrecht, A. Ensminger, P. Arpino, G. Ourisson, *Geochim. Cosmochim. Acta* **38**, 1165 (1974).
4. J. Albaiges, J. Borbón, P. Salagre, *Tetrahedron Lett.* (1978), p. 595 and references cited.
5. M. deRosa, S. deRosa, A. Gambacorta, J. D. Bu'Lock, *J. Chem. Soc. Chem. Commun.* (1977), p. 514.
6. W. K. Seifert and J. M. Moldowan, *Geochim. Cosmochim. Acta* **42**, 77 (1978).
7. Mass spectral fragmentation is preferred at the methyl branches leading to $C_nH_{2n+1}^+$ and $C_nH_{2n}^+$ ions [F. W. McLafferty, *Interpretation of Mass Spectra* (Benjamin, Reading, Mass., ed. 2, 1973)], presumably secondary carbocations in excess of other fragmentations giving primary carbocations.
8. K. B. Wiberg and D. S. Connor, *J. Am. Chem. Soc.* **88**, 4437 (1966).
9. P. Albrecht, personal communication.
10. H. J. Förster, K. Biemann, W. G. Haigh, N. H. Tattrie, J. R. Colvin, *Biochem. J.* **135**, 133 (1973).
11. A. van Dorsselaer, P. Albrecht, G. Ourisson, *Bull. Soc. Chim. Fr.* **5**, 165 (1977).

27 October 1978; revised 18 December 1978

Pleistocene Climate: Deterministic or Stochastic?

Abstract. *Application of a simple linear model to the earth's ice volume record of the past 730,000 years indicates that although forcing by variations in the earth's orbital parameters of tilt and precession is real, it is small (less than 25 percent of the variance in the record). No relationship with the eccentricity is observed. This indicates that the Pleistocene glacial variations are largely stochastic in nature.*

Recently presented geologic evidence (*1*, *2*) strongly supports the astronomical theory of climate change, which states that variations in the seasonal and latitudinal distributions of incoming solar radiation due to long-term variations in the earth's orbital parameters had a significant effect on global climate during the last 2 million years. However, the degree to which the climatic record of glacial and interglacial fluctuations is actually a direct result of orbital controls has not yet been determined (*3*). In addition, the orbital parameters that are expected to have a significant effect on climate are not always those that are actually reflected in the climatic record (*1*). This report addresses these two problems.

The distribution of the sun's energy with respect to latitude is controlled primarily by the tilt of the earth's axis. The distribution of insolation with respect to the seasons is controlled by the precession of the equinox about the sun. Both of these orbital parameters undergo long-term periodic variations caused by the gravitational attraction of other planets in the solar system. Detailed descriptions of these orbital parameters can be found in Chin and Yevjevich (*4*), Broecker and Van Donk (*5*), and Berger (*6*). Based on our precise knowledge of the solar system, the orbital variations have been determined for the past 5 million years, showing that tilt varies with an average period of 41,000 years and precession with an average period of 21,000 years (*6*). The application of spectral analytical techniques to paleoclimatic records obtained from deep-sea cores has identified these periodicities in the record of the earth's climate (*1*, *2*).

In many cases most of the variance of these climatic records is centered at frequencies equal to periods of about 100,000 years. This corresponds to the periodicity of variations in the eccentricity of the earth's orbit. According to the astronomical theory of climate change, however, eccentricity influences the earth's insolation only by modifying the magnitude of the precessional effect.

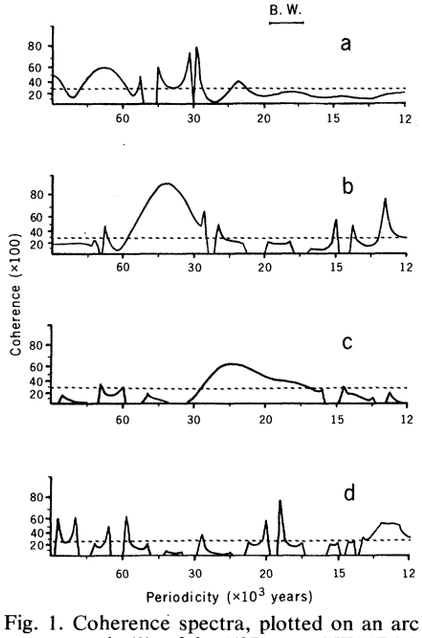

Fig. 1. Coherence spectra, plotted on an arc tangent scale (*9*), of the $\delta^{18}O$ record [TWEAQ time scale (*2*)] with (a) the eccentricity of the earth's orbit, (b) the tilt of the earth's axis, and (c) the precession of the equinox (*6*). The coherence spectrum of the tilt of the earth's axis with the precession of the equinox is shown in (d). All measures of coherence lying below the dashed line are not significantly different from zero at the 80 percent confidence level (16 lags or 20 degrees of freedom). Abbreviation: *B.W.*, bandwidth.

Thus, it should play, at most, a minor role in climatic change (*1*). If we are to understand the exact nature of long-term climatic change it is important to answer the question: How much of this or any other periodic component of the climatic record is attributable to forcing by variations in the earth's orbit?

The problem of the degree to which the climate of the late Pleistocene is either stochastic or deterministic has been approached by a number of authors. Hays *et al.* (*1*) assumed that all the variance in the peaks in the power spectrum of their climatic record, which correspond to the periodicities of precession, obliquity, and eccentricity, could be attributed to forcing. As a result, they concluded that about 80 percent of the variance in their 450,000-year climatic record was due to orbital forcing. Chin and Yevjevich (*4*) presented a mathematical model for long-term changes in the world's ice volume and described climate change as "an almost periodic stochastic process." They concluded that 59 percent of the variation in global ice volume is stochastic.

If variations in tilt and precession are the primary causes of climatic variation, we can calculate the deterministic component of the ice volume record through the use of a two-input, single-output linear time series model. This model considers two input time series $x_1(t)$ and $x_2(t)$ and one output $y(t)$. To get an estimate of the degree to which the output series is controlled by the input series, the pooled coherence function $C^2_{x_1x_2y}(f)$ is required (*7*). This function, which ranges in value from 0 to 1, is analogous to a simple squared correlation coefficient in that its value at a particular frequency f_0 indicates the amount of the variance contained in $y(t)$ at that frequency that can be explained in terms of simple forcing by $x_1(t)$ and $x_2(t)$. If $x_1(t)$ and $x_2(t)$ are independent—that is, if the coherence between them is zero for all frequencies—the expression for the total coherence function for $y(t)$ and both $x_1(t)$ and $x_2(t)$ is

$$C^2_{x_1x_2y}(f) = C^2_{x_1y}(f) + C^2_{x_2y}(f) \quad (1)$$

where $C^2_{x_1y}$ and $C^2_{x_2y}$ are the coherences of $y(t)$ with $x_1(t)$ and $x_2(t)$, respectively (*8*). The spectrum of the estimated output function $S_{x_1x_2y}$ is obtained from the product of the spectrum of $y(t)$, S_y, and the pooled squared coherence $C^2_{x_1x_2y}$

$$S_{x_1x_2y}(f) = S_y(f)\, C^2_{x_1x_2y}(f)$$

The integral of this function gives the amount of variance in $y(t)$ explained by the model.

0036-8075/79/0413-0171$00.50/0